Thermochimica Acta 318 (1998) 165–175

thermochimica
acta

Thermal and structural studies of amide complexes of transition metal(II) chlorides. I: Stoichiometry

Aubrey N. Nelwamondo[a], Desmond J. Eve[b], Gareth M. Watkins[b], Michael E. Brown[b,*]

[a] *Department of Chemistry, University of Fort Hare, Alice, South Africa*
[b] *Department of Chemistry, Rhodes University, Grahamstown, 6140, South Africa*

Received 15 July 1997; accepted 2 September 1997

Abstract

A series of aliphatic amide complexes of nickel(II), cobalt(II) and copper(II) chlorides has been prepared. These complexes have the general formulae: $NiL_2Cl_2 \cdot 2H_2O$, NiL_2Cl_2, $Ni_3L_2Cl_6$, Ni_3LCl_6, CoL_2Cl_2 and CuL_2Cl_2, where L is the amide ligand. Ligands ranging from formamide to butyramide, both with and without *N*-methyl and *N*-ethyl substituents, were used. The complexes were found, from the absorption spectra, to be octahedral or distorted-octahedral, except for some of the cobalt complexes with dimethyl substituted ligands which are tetrahedral. Infrared spectra confirm that coordination to the metal ion is through the carbonyl oxygen. The effects of the structure and the nature of the different amide ligands on the thermal stabilities of the complexes have been investigated by thermal analysis. As indicators of the stability of the metal–amide binding, thermal decomposition onset temperatures (T_e), peak temperatures (T_{max}) and enthalpies (ΔH_L) were compared for complexes with similar composition, geometrical structure and decomposition stoichiometry. Results do not support the enhancement of thermal quantities with increasing basicity of the amides. Instead, steric factors appear to play a more important role in determining the magnitudes of ΔH_L, T_e and T_{max} © 1998 Elsevier Science B.V.

Keywords: Amide complexes; Nickel(II); Cobalt(II); Copper(II); Structure; Thermal analysis

1. Introduction

Thermochemical, kinetic, spectroscopic and stability correlation studies of solid metal halide complexes have been the subject of several investigations [1–10]. In such studies, attempts have often been made to relate thermal decomposition parameters such as T_e (the procedural decomposition onset temperature), T_{max} (peak temperature), ΔH (change in enthalpy) and E_a (apparent activation energy) to the strengths of metal-volatile ligand bonds, structure and IR properties.

The organic ligands that have attracted most interest in thermal decomposition studies of metallo-organic complexes have been nitrogen donor molecules, particularly pyridine and its alkyl-substituted derivatives, as well as imidazoles. Reports on metallo-amide complexes are limited [11–13]. The monoligand complexes of type MLX_2 (where M is a transition metal, X a halogen and L a simple amide) cannot be readily prepared, with the result that there have been no systematic investigations of the monoligand com-

---

*Corresponding author. Tel.: +27 46 6038254; fax: +27 466225109; e-mail: chmb@warthog.ru.ac.za

0040-6031/98/$19.00 © 1998 Elsevier Science B.V. All rights reserved
PII S0040-6031(98)00341-4

plexes. The first examples of nickel(II) chloride complexes containing one amide ligand for each nickel ion have been prepared in this study. We have also prepared new complexes of the types: $NiL_2Cl_2{\cdot}H_2O$, ML_2Cl_2 (where M=Ni, Co, Cu), $Ni_3L_2Cl_6$ and Ni_3LCl_6. Elemental analyses and spectral and thermogravimetric measurements were used to characterize the complexes.

The amides ligands (L) used in this study are of the general structural formula

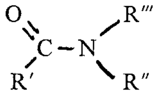

where R′ is H, or an alkyl group such as methyl, ethyl or propyl. R″ and R‴ are H's, or groups such as methyl or ethyl, or one of these groups and hydrogen. Those used were: acetamide, *aa*, (C_2H_5NO); *N*-methylacetamide, *nma*, (C_3H_7NO); *N*, *N*-dimethylacetamide, *dma*, (C_4H_9NO); formamide, *fa*, (CH_3NO); *N*-methylformamide, *nmf*, (C_2H_5NO); *N*, *N*-dimethylformamide, *dmf*, (C_3H_7NO); *N*-ethylformamide, *nef*, (C_3H_7NO); *N*, *N*-diethylformamide, *def*, ($C_5H_{11}NO$); propionamide, *pa*, (C_3H_7NO); butyramide, *ba*, (C_4H_9NO); isobutyramide, *iba*, (C_4H_9NO) and (*N*, *N*-dimethylpropionamide, *dmp*, ($C_5H_{11}NO$).

Possible relationships between the strengths of the metal-amide bonds (of complexes prepared from a homologous series of amide ligands), the thermal decomposition parameters, and spectroscopic properties have been investigated. Variation of the alkyl constituents, i.e. methyl, ethyl or propyl, in the amide skeleton makes it possible to investigate the steric and inductive effects. It has been shown [14–16] that coordination to the metal ion generally occurs through the oxygen of the amide molecule in this type of complex, and this coordination has been confirmed in this study.

The use of the procedural onset temperature (T_e), the peak temperature (T_{max}) and the enthalpy change (ΔH) of decomposition as characteristic measures of the strengths of the metal–volatile ligand bonds is not universally accepted, so in Part 2 of this study [17] apparent activation energies, E_a, which have been proposed [3–6,10,18–20] as the parameters that are more closely connected with the strengths of the broken bonds, were determined where possible and similarly assessed.

2. Experimental

2.1. Preparation of complexes

Two standard methods were used to prepare the complexes [12,21]. Method A consisted of a mixture of boiling ethanol solutions of the metal(II) chloride and the amide in 1:2 molar ratio. The precipitated complex was washed with dry ether and then dried in a desiccator over P_2O_5. The complexes were recrystallized from a 1:1 mixture of anhydrous ethanol and ether.

Method B involved isothermal heating of an appropriate complex, prepared as above, at a temperature suitable to yield a complex of the required composition.

2.2. Elemental analyses

Metal contents were determined using atomic absorption analysis (Unicam-939 AA spectrophotometer). Carbon, hydrogen and nitrogen analyses were performed using a Carlo-Erba Microanalyzer. Results are given in Table 1.

2.3. Thermal measurements

Thermal decomposition studies were carried out using thermogravimetry (TG) and differential scanning calorimetry (DSC) on Perkin–Elmer Series-7 instruments. Open platinum crucibles were used for TG and covered, but not crimped, aluminium pans for DSC. The flow rate of high purity nitrogen was about 20 $cm^3\ min^{-1}$.

2.4. Spectral measurements

Solid diffuse reflectance (Beckman 5240) and FT–IR spectra (Perkin–Elmer 2000 System; KBr discs 250–400 cm^{-1} and CsI discs 500–200 cm^{-1}) were recorded for all the starting complexes, intermediate complexes formed during thermal decomposition, and the final decomposition product. Results are given in Table 2.

3. Results and discussion

3.1. Stoichiometries

The complexes were prepared and their analytical data are given in Table 1. The amounts of ligand were

Table 1
Analytical data for the complexes

Preparation method	Complex stoichiometry	% Metal found (calculated)*	% Nitrogen found (calculated)	% Carbon found (calculated)	% Hydrogen found (calculated)	% Ligand found (calculated)
(a) $NiL_2Cl_2\cdot 2H_2O$						
A	$Ni(nmf)_2Cl_2\cdot 2H_2O$	19.6 (20.7)	10.3 (9.9)	17.7 (16.9)	4.7 (5.0)	55.6 (54.3)
A	$Ni(aa)_2Cl_2\cdot 2H_2O$	22.0 (20.7)	9.5 (9.9)	16.3 (16.9)	4.6 (5.0)	54.8 (54.3)
A	$Ni(nma)_2Cl_2\cdot 2H_2O$	20.1 (18.8)	9.4 (9.0)	22.2 (23.1)	6.0 (5.8)	57.9 (58.4)
(b) $NiLCl_2$						
B	$Ni(nmf)Cl_2$	32.4 (31.1)	7.3 (7.4)	12.4 (12.7)	2.6 (2.7)	32.2 (31.3)
B	$Ni(aa)Cl_2$	31.4 (31.1)	6.8 (7.4)	11.7 (12.7)	2.6 (2.7)	30.8 (31.3)
B	$Ni(nma)Cl_2$	29.3 (29.0)	6.6 (6.9)	16.8 (17.8)	3.5 (3.5)	35.8 (36.1)
(c) NiL_2Cl_2						
A	$Ni(fa)_2Cl_2$	25.2 (26.7)	12.6 (12.8)	10.9 (10.9)	2.8 (2.8)	40.7 (41.0)
A	$Ni(dmf)_2Cl_2$	19.4 (21.3)	9.7 (10.2)	26.3 (26.1)	5.1 (5.1)	54.7 (53.0)
A	$Ni(nef)_2Cl_2$	19.3 (21.3)	9.8 (10.2)	25.4 (26.1)	5.2 (5.1)	53.5 (53.0)
A	$Ni(pa)_2Cl_2$	20.8 (21.3)	10.0 (10.2)	26.0 (26.1)	5.3 (5.1)	53.5 (53.0)
A	$Ni(ba)_2Cl_2$	17.5 (19.3)	8.0 (9.2)	28.0 (31.6)	5.8 (6.0)	56.9 (57.3)
A	$Ni(iba)_2Cl_2$	16.9 (19.3)	8.2 (9.2)	28.2 (31.6)	5.8 (6.0)	55.7 (57.3)
(d) $Ni_3L_2Cl_6$						
B	$Ni_3(dmf)_2Cl_6$	32.4 (32.9)	5.0 (5.2)	13.1 (13.5)	2.8 (2.6)	27.0 (27.3)
A	$Ni_3(dma)_2Cl_6$	33.2 (32.9)	5.8 (5.0)	18.1 (17.1)	3.7 (3.2)	29.7 (30.9)
A	$Ni_3(def)_2Cl_6$	31.4 (32.6)	4.6 (4.7)	19.3 (20.3)	3.8 (3.8)	34.7 (34.2)
B	$Ni_3(nef)_2Cl_6$	31.9 (32.9)	5.2 (5.2)	14.8 (13.5)	3.1 (2.6)	28.9 (27.3)
B	$Ni_3(pa)_2Cl_6$	32.5 (32.9)	14.9 (5.2)	12.3 (13.5)	2.7 (2.6)	27.6 (27.3)
(e) Ni_3LCl_6						
A	$Ni_3(dmp)Cl_6$	36.6 (35.9)	4.6 (4.7)	17.2 (20.3)	3.6 (3.8)	21.9 (20.6)
(f) CoL_2Cl_2						
A	$Co(fa)_2Cl_2$	27.4 (26.8)	12.6 (12.7)	10.8 (10.9)	2.8 (2.8)	41.6 (41.0)
A	$Co(nma)_2Cl_2$	20.5 (21.4)	9.7 (10.2)	25.0 (26.1)	5.2 (5.1)	52.0 (53.0)
A	$Co(dmf)_2Cl_2$	19.5 (21.4)	8.6 (10.2)	25.6 (26.1)	5.1 (5.1)	53.4 (53.0)
A	$Co(dma)_2Cl_2$	19.1 (19.4)	9.1 (9.2)	31.3 (31.6)	6.0 (6.0)	57.7 (57.3)
A	$Co(dmp)_2Cl_2$	18.1 (18.7)	6.9 (8.4)	23.0 (18.1)	4.2 (3.3)	57.1 (60.9)
(g) CuL_2Cl_2						
A	$Cu(aa)_2Cl_2$	25.1 (25.2)	10.4 (11.1)	17.8 (19.0)	3.8 (4.0)	47.3 (46.8)
A	$Cu(fa)_2Cl_2$	27.1 (28.4)	12.0 (12.5)	10.5 (10.7)	2.7 (2.7)	43.0 (40.1)
A	$Cu(iba)_2Cl_2$	22.4 (20.6)	8.6 (9.1)	30.2 (31.1)	5.8 (5.9)	54.5 (56.4)

determined from TG mass loss data. The analytical compositions found are in reasonable agreement with the calculated values.

3.2. Structures of complexes

Visible and near-infrared reflectance spectra of the various complexes (Table 2) were used to study the geometrical configuration of the metal(II) ions. Spectra of the $NiCl_2$–amide complexes are similar to those of the related nickel(II) chloride complexes reported by other workers [12,13,21–24].

The ligands (L) in $NiL_2Cl_2\cdot 2H_2O$ were *nmf*, *nma* or *aa*. Thermoanalytical curves indicated that loss of water occurs below 120°C. This infers that the water molecules are held outside the coordination sphere [9,11,25]. Isothermal heating yielded corresponding complexes of the type $NiLCl_2$. Visible and near-infrared reflectance spectra suggest octahedral coordination of the metal ion.

Ligands *nef*, *dmf*, *fa*, *pa*, *ba* and *iba* yielded complexes of the type NiL_2Cl_2 from their respective ethanol solutions. Two forms of octahedral arrangement are suggested by the visible and near-infrared spectra of the NiL_2Cl_2 complexes (Table 2).

Table 2
Diffuse reflectance spectra of the amide complexes of (a) nickel(II) chloride (b) cobalt(II) chloride (c) copper(II) chloride

Complex	Colour	Band assignments/10^3 cm^{-1}		
		$^3T_{2g}(F) \leftarrow {}^3A_{2g}(F)$	$^3T_{1g}(F) \leftarrow {}^3A_{2g}F)$	$^3T_{1g}(P) \leftarrow {}^3A_{2g}(F)$
$NiCl_2$	Brown	7.223	11.696; 12.826	22.222
(i) *$NiLCl_2$*				
$\mathrm{Ni}(\mathit{nmf})\mathrm{Cl_2}$	Brown	7.249	11.838	22.388
$\mathrm{Ni}(\mathit{aa})\mathrm{Cl_2}$	Brown	7.238	11.413	22.089
$\mathrm{Ni}(\mathit{nma})\mathrm{Cl_2}$	Brown	7.236	11.415	22.028
(ii) *$NiL_2Cl_2 \cdot 2H_2O$*				
$\mathrm{Ni}(\mathit{nmf})2\mathrm{Cl_2 \cdot 2H_2O}$	Orange	7.249	11.780	22.329
$\mathrm{Ni}(\mathit{aa})_2\mathrm{Cl_2 \cdot 2H_2O}$	Orange	7.267	11.846	22.477
$\mathrm{Ni}(\mathit{nma})_2\mathrm{Cl2 \cdot 2H_2O}$	Orange	7.252	12.124	23.371
(iii) *$Ni_3L_2Cl_6$*				
$\mathrm{Ni_3}(\mathit{dmf})_2\mathrm{Cl_6}$	Brown	7.259	11.701	22.047
$\mathrm{Ni_3}(\mathit{dma})_2\mathrm{Cl_6}$	Brown	7.252	11.627	21.989
$\mathrm{Ni_3}(\mathit{nef})_2\mathrm{Cl_6}$	Brown	7.232	11.531	21.885
$\mathrm{Ni_3}(\mathit{pa})_2\mathrm{Cl_6}$	Brown	7.221	11.375	21.770
$\mathrm{Ni_3}(\mathit{def})_2\mathrm{Cl_6}$	Brown	7.247	11.586	21.738
(iv) *NiL_2Cl_2*				
$\mathrm{Ni}(\mathit{fa})_2\mathrm{Cl_2}$	Intense-orange	7.286	11.885	22.311
$\mathrm{Ni}(\mathit{dmf})_2\mathrm{Cl_2}$	Intense-orange	7.267	12.556	23.077
$\mathrm{Ni}(\mathit{nef})_2\mathrm{Cl_2}$	Blue–green	7.271	14.167;15.200	22.074
$\mathrm{Ni}(\mathit{pa})_2\mathrm{Cl_2}$	Blue–green	7.556	14.196;15.334	23.280
$\mathrm{Ni}(\mathit{ba})_2\mathrm{Cl_2}$	Blue–green	7.460	14.328;15.236	21.985
$\mathrm{Ni}(\mathit{iba})_2\mathrm{CR_2}$	Blue–green	7.258	14.279;15.243	21.985
(v) *Ni_3LCl_6*				
$\mathrm{Ni_3}(\mathit{dmp})\mathrm{Cl_6}$	Brown	7.285	11.739	21.744
(i) Octahedral		$^4T_{2g}(F) \leftarrow {}^4T_{1g}(F)$	$^4A_{2g}(F) \leftarrow {}^4T_{1g}(F)$	$^4T_{1g}(P) \leftarrow {}^4T_{1g}(F)$
$CoCl_2$	Blue	6.291	12.980	16.892
$\mathrm{Co}(\mathit{fa})_2\mathrm{Cl_2}$	Mauve	5.808	13.356	16.112(sh); 19.299
$\mathrm{Co}(\mathit{nma})_2\mathrm{CR_2}$	Blue	6.293	11.933	15.567;18.573(sh)
(ii) Tetrahedral		$^4T_1(F) \leftarrow {}^4A_2(F)$		$^4T(P) \leftarrow {}^4A_2(F)$
$\mathrm{Co}(\mathit{dmf})_2\mathrm{Cl_2}$	Royal blue	6.110		15.024
$\mathrm{Co}(\mathit{dma})_2\mathrm{Cl_2}$	Royal blue	5.880		15.172;19.588(sh)
$\mathrm{Co}(\mathit{dmp})_2\mathrm{Cl_2}$	Royal blue	5.880		15.172
Octahedral		Observed bands/10^3 cm^{-1} $^2T_{2g} \leftarrow {}^2E_g$		
$CuCl_2$	Buff	13.057		24.404
$\mathrm{Cu}(\mathit{aa})\mathrm{Cl_2}$	Green	12.969		—
$\mathrm{Cu}(\mathit{fa})_2\mathrm{Cl_2}$	Green	13.018		—
$\mathrm{Cu}(\mathit{iba})_2\mathrm{Cl_2}$	Gold	11.930		26.325

$\mathrm{Ni}(\mathit{fa})_2\mathrm{Cl_2}$ and $\mathrm{Ni}(\mathit{dmf})_2\mathrm{Cl_2}$ have an intense orange colour and their spectra are similar to most of the other nickel complexes prepared and anhydrous $NiCl_2$ (which are brown or orange), i.e. typical of low-field octahedral nickel(II) compounds. The spectra of the NiL_2Cl_2 complexes, where L is *pa, nef, ba* or *iba*, all have a broad, multi-component, centre band, corresponding to the ν_2 transition of other complexes, which suggests that some distortion of the structure is present. Their spectra are similar to those of the related nickel(II)–amide complexes reported by other workers [12,13,21] for which additional evidence was used to support octahedral coordination. Chloride bridges are anticipated, and the octahedra proposed may have some D_{2h} symmetry character. Other authors [26–31] have suggested that splitting of the ν_1 (and ν_2) transitions may results from a tetragonal distortion leading to a symmetry approaching D_{4h}. No ν_1 split was evident from the visible region reflectance spectra recorded in this study.

Upon heating at selected constant temperatures NiL_2Cl_2 (where L=*nef*, *dmf* or *pa*) yielded complexes of the type $Ni_3L_2Cl_6$. Similar complexes were prepared from ethanol solutions for *def* and *dma* ligands. Ni_3(*dmp*)Cl_6 was the only complex of the type Ni_3LCl_6 characterized.

Diffuse reflectance spectra of the mauve Co(*fa*)$_2$Cl$_2$ and the blue Co(*nma*)$_2$Cl$_2$, Table 2, suggest an octahedral environment for cobalt(II) ions. The spectra are similar to the spectrum of anhydrous $CoCl_2$. The ratio of $\nu_2/\nu_1 \approx 2.0$ conforms to the usual value from octahedral assignment [25]. Spectra of Co(*dmf*)$_2$Cl$_2$, Co(*dma*)$_2$Cl$_2$ and Co(*dmp*)$_2$Cl$_2$ (Table 2) are typical of cobalt(II) ion in a tetrahedral environment. The Co(*dma*)$_2$Cl$_2$ complex isolated by Madan et al. [32] also exhibited tetrahedral coordination.

The visible region reflectance spectra of the CuL_2Cl_2 complexes (where L=*fa*, *aa* or *iba*) show a broad band around 13 000 cm^{-1} (Table 2). This suggests octahedral coordination. Cu(*iba*)$_2$Cl$_2$ and $CuCl_2$ show a second band at higher frequency which is probably not associated with a d–d transition.

The frequencies of the IR absorption band assignments indicated a negative shift of the carbonyl stretch (about 8–45 cm^{-1}) and a positive shift of the ν_{C-N} stretch (about 8–60 cm^{-1}) on complex formation. The $\Delta_{C=O}$ and Δ_{C-N} values (Table 3) are compared favourably with similar values reported by other workers [27,33–35]. The amide ligands are thus coordinated to the metal(II) ion through the carbonyl oxygen atom. Tentative assignments of ν_{M-Cl} and ν_{M-O} absorption bands are shown in Table 3. The ν_{M-Cl} stretching vibrations were assigned following (primarily) related reports [23,24,28–31,36–38]. The assignments have been notably assisted by observing: (i) the halogen sensitivity of some of the bands, and (ii) the effects of varying the amide ligand in the complex. Two strong ν_{M-Cl} bands are expected due to MCl_2 stretches. If the ν_{M-X} bands separation reported by Dorrity et al. [38] are assumed to hold for the present series of amide complexes, then the assignment of one ν_{M-Cl} is consistent with the reports that other bridging ν_{M-X} often appear below 200 cm^{-1} [28,30,39]. Such bands fall outside the lower frequency range of the detector (mirTGS) used.

The actual structures of the various octahedral metal(II) chloride complexes are not known, but it is postulated that there is considerable chloride bridging. The assignments of the ν_{M-Cl} vibrations are in agreement with assignments made for similar vibrations in related complexes [40–43] for which halide bridging has been suggested.

3.3. Thermal behaviour and reaction stoichiometries

The thermal decomposition stoichiometries and enthalpies of reaction of all the analytically characterized complexes were determined from TG and DSC curves. Complexes which clearly exhibited melting were not considered for kinetic measurements (Part 2, [17]).

The $NiL_2Cl_2 \cdot 2H_2O$ complexes decomposed in two or three endothermic steps. The loss of the first amide ligand follows dehydration (illustrated for Ni(*nmf*)$_2$Cl$_2$·2H$_2$O in Fig. 1), but attempts to isolate a NiL_2Cl_2 intermediate were unsuccessful. The DTG curve of the Ni(*nma*)$_2$Cl$_2$·2H$_2$O complex (Fig. 2) indicates a simultaneous loss of $2H_2O$ and the first *nma* molecule, while the DSC curve shows three endothermic stages. All three complexes decomposed via the formation of stable $NiLCl_2$ intermediates which were isolated and characterized.

TG, DTG and DSC curves of the $NiLCl_2$ complexes (illustrated for Ni(*nmf*)Cl$_2$ in Fig. 3) indicate that the ligand L is removed completely in a single endothermic step.

The thermoanalytical curves of the NiL_2Cl_2 complexes (illustrated for Ni(*ba*)$_2$Cl$_2$ in Fig. 4) indicate two decomposition steps which overlap partially for some of the complexes. The DSC curves indicate complex overlapping endotherms. The sharpness of the first DSC endotherm (Fig. 4) suggests melting. Hot-stage microscopy and visual inspection of larger

Table 3
Summary of the IR frequencies ($\nu_{M\text{–}O}$ and $\nu_{M\text{–}Cl}$) and the ligand frequency shifts on complexation ($\Delta\nu_{C=O}$ and$\Delta\nu_{C\text{-}N}$) for the MCl_2–amide complexes

Ligand (L) in	$\nu_{M\text{–}O}$/(cm^{-1})	$\nu_{M\text{–}Cl}$/(cm^{-1})	$\Delta\nu_{C=O}$/(cm^{-1})	$\Delta\nu_{C\text{–}N}$/(cm^{-1})
(a) *NiLCl*$_2$				
nmf	367	226	−13	47
aa	357	220	−24	60
nma	366	225	−26	11
(b) *NiL*$_2$*Cl*$_2$*.2H*$_2$*O*				
nmf	368	226	−516	15
aa	380	222	−21	66
nma	353	225	−30	8
(c) *Ni*$_3$*L*$_2$*Cl*$_6$				
dmf	402	220	−18	18
dma	346	224	−19	2
nef	398	222	−14	23
pa	351	223	−9	50
def	396	223	−29	12
(d) *NiL*$_2$*Cl*$_2$				
dmf	393	233	−23	23
nef	397	221	−20	7
fa	352	222	3	36
pa	360	228	−8	51
ba	397	223	−15	41
iba	377	219	−18	50
e) *Ni*$_3$*(dmp)Cl*$_6$	346	216	−41	9
(f) *CoL*$_2$*Cl*$_2$				
nma	351	224	−27	13
dmf	311	247	−20	19
fa	313	225	1	36
dma	305	248	−22	27
dmp	304	248	−44	13
(g) *CuL*$_2$*Cl*$_2$				
aa	352	226	−19	52
fa	—	232	5	57
iba	399	221	−20	50

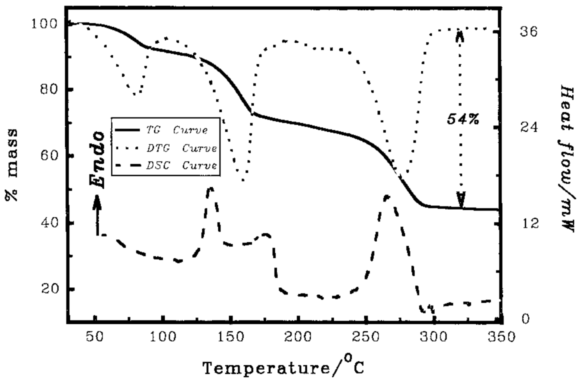

Fig. 1. TG, DTG and DSC curves for Ni(*nmf*)$_2$Cl$_2$.2H$_2$O heated at 20 K min^{-1} in flowing N$_2$.

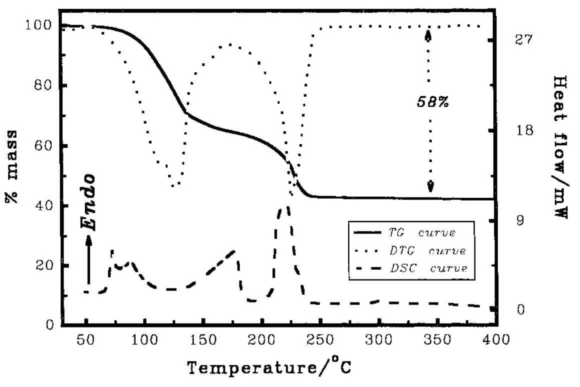

Fig. 2. TG, DTG and DSC curves for Ni(*nma*)$_2$Cl$_2$.2H$_2$O heated at 20 K min^{-1} in flowing N$_2$.

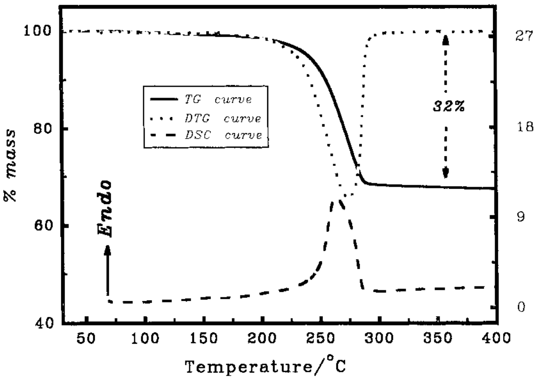

Fig. 3. TG, DTG and DSC curves for Ni(*nmf*)Cl_2 heated at 20 K min^{-1} in flowing N_2.

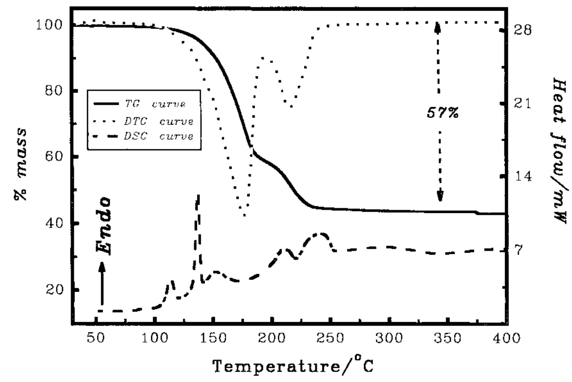

Fig. 4. TG, DTG and DSC curves for Ni(*ba*)$_2Cl_2$ heated at 20 K min^{-1} in flowing N_2.

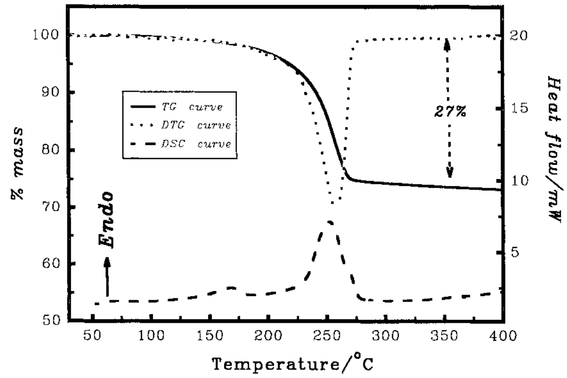

Fig. 5. TG, DTG and DSC curves for Ni_3(*dmf*)$_2Cl_6$ heated at 20 K min^{-1} in flowing N_2.

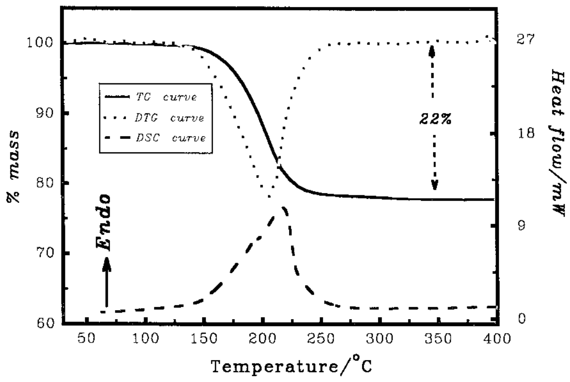

Fig. 6. TG, DTG and DSC curves for Ni_3(*dmp*)Cl_6 heated at 20 K min^{-1} in flowing N_2

quantities of samples of the partially decomposed complexes with L=*iba, ba, pa* or *nef* confirmed melting. TG mass losses for the first step were consistent with the formation of $Ni_3L_2Cl_6$ intermediate. Some $Ni_3L_2Cl_6$ intermediates were isolated and characterized.

Thermoanalytical curves of the $Ni_3L_2Cl_6$ complexes (illustrated for Ni_3(*dmf*)$_2Cl_6$ in Fig. 5) indicate that the ligands are removed completely in a single endothermic step. Decomposition of the only Ni_3LCl_6 complex, Ni_3(*dmp*)Cl_6, occurs in an endothermic single-stage loss of *dmp* to give $NiCl_2$ residue (Fig. 6).

The thermal decomposition patterns of the nickel(II)–amide complexes are in accordance with the experience of other workers [21,25,44–47]. There are however, two important differences concerning the $NiL_2Cl_2 \cdot 2H_2O$ complexes: (i) the $NiLCl_2$ intermediate isolated by Mitra et al. [25] had a T_d symmetry, and (ii) transformed to $NiCl_2$ via two further intermediates.

$CoCl_2$–amide complexes of similar composition and geometrical structure showed different thermal behaviour. The octahedral Co(*fa*)$_2Cl_2$ decomposed (in the solid state) via the formation of Co(*fa*)Cl_2, whilst Co(*nma*)$_2Cl_2$ decomposed (from a molten state) in a single step to give $CoCl_2$. The tetrahedral complexes with *dmf* or *dma* form Co_3(*dmf*)$_2Cl_6$ and Co_3(*dma*)Cl_6 species (respectively) from melts. Co(*dmp*)$_2Cl_2$ decomposed (from a molten state) in a single step to give $CoCl_2$. The reaction stoichiometries differ from those of the corresponding nickel(II) chloride complexes, except for the complex of cobalt(II) with *dmf*. There are, however, two notable differences: (i) no signs of melting were detected in Ni(*dmf*)$_2Cl_2$, and (ii) Co(*dmf*)$_2Cl_2$ has a tetrahedral structure whilst Ni(*dmf*)$_2Cl_2$ is octahedrally coordinated. The single-stage (liquid phase) loss of 2L molecules from related CoL_2Cl_2 complexes has been reported by other workers [45,48,49]. Intermediates of type $CoLCl_2$ have also been suggested [12,50,51].

$CuCl_2$–amide complexes of similar composition and structure to the Ni(II) complexes showed different thermal behaviour. The Cu(*fa*)$_2$Cl$_2$ and Cu(*aa*)$_2$Cl$_2$ complexes decomposed (from a molten state) via the formation of $CuLCl_2$ species. Cu(*iba*)$_2$Cl$_2$ decomposed (from the melt) in a single step to give a molten product. Similar behaviour has been reported for related copper(II) complexes [13,48,49].

The thermal decompositions of the amide complexes can be summarized by the following sets of reactions:

$$\text{Set 1}: ML_2Cl_2(s) \rightarrow MLCl_2(s) + L(g) \quad (1)$$

$$MLCl_2(s) \rightarrow MCl_2(s) + L(g) \quad (2)$$

$$\text{Set 2}: 3ML_2Cl_2(s) \rightarrow M_3L_2Cl_6(s) + 4L(g) \quad (3)$$

$$M_3L_2Cl_6(s) \rightarrow 3MCl_2(s) + 2L(g) \quad (4)$$

$$\text{Set 3}: 3ML_2Cl_2(s) \rightarrow M_3LCl_6(s) + 5L(g) \quad (5)$$

$$M_3LCl_6(s) \rightarrow 3MCl_2(s) + L(g) \quad (6)$$

$$\text{Set 4}: ML_2Cl_2(s) \rightarrow MCl_2(s) + 2L(g) \quad (7)$$

T_e and T_{max} (for the first decomposition steps) were determined from the DTG curves, and ΔH_{zL} from the DSC curves. Values of the stoichiometric coefficient (z) of the released ligands and the measured enthalpy change were used to calculate the enthalpy per mole of the amide ligand. Evaluation of ΔH_{zL} for the individual decomposition steps in some of the reactions proved difficult owing to the overlap of the DSC stages. This problem was overcome by estimating ΔH_L values on the basis of the release of all ligands, irrespective of the number of steps in a thermal process. Results are shown in Table 4.

4. Discussion

4.1. The influence of the nature of the amide ligands on the thermal stabilities of their corresponding metal(II) complexes

One of the primary objectives of this work was to investigate the possible relationship between the nature of the amides (steric and electronic effects) and the thermal stabilities of their corresponding metal(II) chloride complexes. As indicators of the stability of the metal–amide binding, thermal decomposition onset temperatures (T_e), peak temperatures (T_{max}) and enthalpies (ΔH_L) were compared for complexes with similar composition, geometrical structure and decomposition stoichiometry.

4.1.1. Reactions of Set (1)

Thermal data for reaction 1b, Table 4, indicate the orders of $NiLCl_2$: (i) T_e *nma*<*aa*<*nmf*; (ii) T_{max} *nma*<*aa*<*nmf*; (iii)ΔH_L *nma*<*aa*< *nmf*. These sequences are consistent and reflect the order of decreasing steric hindrance of the methyl-substituent groups. The least stable complex, as suggested by the smallest values of ΔH_L, T_e and T_{max}, is Ni(*nma*)Cl$_2$. This could be explained in terms of steric interaction where the double methyl group attached to the carbonyl carbon atom hinders the effective interaction of the central nickel(II) ion with the carbonyl oxygen atom. If inductive effects were more important than steric effects, Ni(*nmf*)Cl$_2$ would come below Ni(*aa*)Cl$_2$ in the stability series. Less steric repulsion is expected from less bulky amides, leading to stronger interaction with the metal and higher frequencies of the $^3T_2g(F) \leftarrow {}^3A_2g(F)$ transition (ν_1) [8,22,52]. The shift of the ν_1 band to higher wavenumbers (Table 2) produced the sequence: *nma* (7236 cm^{-1}) ≅*aa* (7238 cm^{-1})<*nmf* (7249 cm^{-1}).

This sequence is consistent with the steric hindrance caused by the methyl-substituent groups. The difference in the ν_1 values for the Ni(*aa*)Cl$_2$ and Ni(*nma*)Cl$_2$ complexes is however, not well established.

Assuming that a higher IR carbonyl frequency band shift confirms a stronger inductive effect, $\Delta\nu_{C=O}$ should increase from *nmf* to *nma* in accordance with the expected increase in bond order. The $\Delta\nu_{C=O}$ values in Table 3 confirm this order. That is, *nmf* (13 cm^{-1})<*aa* (24 cm^{-1}) ≅ *nma* (26 cm^{-1}).

In the $NiLCl_2$ system, the quantities ΔH_L, T_e and T_{max} thus indicate a stronger influence of the steric rather than the inductive effects. Thermal data for reactions Eqs. (1) and (2), Table 4, indicate the orders of $NiL_2Cl_2 \cdot 2H_2O$: (i)T_e *nmf*<*aa*; (ii)T_{max} *nmf*<*aa*; (iii)ΔH_L *aa*<*nmf*; and of CuL_2Cl_2: (i)T_e *aa*<*fa*; (ii)T_{max} *aa*<*fa*.

Table 4
Summary of thermal data for the various metal(II)–amide complexes

Complex	Reaction	T_e/(°C)	T_{max}/(°C)	ΔH_L/kJ mol^{-1} ligand
(a) $NiLCl_2$				
Ni(*nmf*)Cl$_2$	Eq. (2)	243	271	67
Ni(*aa*)Cl$_2$	Eq. (2)	228	244	63
Ni(*nma*)Cl$_2$	Eq. (2)	215	230	60
(b) $NiL_2Cl_2{\cdot}2H_2O$				
Ni(*nmf*)$_2$Cl$_2$·2H$_2$O	Eqs. (1) and (2)	136	148	74
Ni(*aa*)$_2$Cl$_2$·2H$_2$O	Eqs. (1) and (2)	197	215	66
Ni(*nma*)$_2$C l$_2$·2H$_2$O	Eqs. (1) and (2)	—	—	—
(c) $Ni_3L_2Cl_6$				
Ni$_3$(*dmf*)$_2$Cl$_6$	Eq. (4)	217	259	51
Ni$_3$(*dma*)$_2$Cl$_6$	Eq. (4)	239	248	46
Ni$_3$(*nef*)$_2$Cl$_6$	Eq. (4)	250	274	47
Ni$_3$(*pa*)$_2$Cl$_6$	Eq. (3)	182	207	46
Ni$_3$(*def*)$_2$Cl$_6$	Eq. (4)	200	229	45
(d) NiL_2Cl_2				
Ni(*fa*)$_2$Cl$_2$	Eqs. (3) and (4)	233	256	69
Ni(*dmf*)$_2$Cl$_2$	Eqs. (3) and (4)	89	107	64
Ni(*nef*)$_2$Cl$_2$	Eqs. (3) and (4)	144	168	53
Ni(*pa*)$_2$Cl$_2$	Eqs. (3) and (4)	153	179	50
Ni(*ba*)$_2$Cl$_2$	Eqs. (3) and (4)	163	191	42
Ni(*iba*)$_2$Cl$_2$	Eqs. (3) and (4)	158	198	40
(e) Ni_3LCl_6				
Ni$_3$(*dmp*)Cl$_6$	Eq. (6)	176	206	61
(f) CoL_2Cl_2				
Co(*fa*)$_2$Cl$_2$	Eqs. (1) and (2)	194	221	68
Co(*nma*)$_2$Cl$_2$	Eq. (7)	217	248	—
(g)CoL_2Cl_2				
Co(*dmf*)$_2$Cl$_2$	Eqs. (3) and (4)	106	192	—
Co(*dma*)$_2$Cl$_2$	Eqs. (5) and (6)	202	245	—
Co(*dmp*)$_2$Cl2	Eq. (7)	210	240	—
(h)CuL_2Cl_2				
Cu(*aa*)$_2$Cl$_2$	Eqs. (1) and (2)	165	191	—
Cu(*fa*)$_2$Cl$_2$	Eqs. (1) and (2)	182	205	—
Cu(*iba*)$_2$Cl$_2$	Eq. (7)	193	220	—

In the NiL$_2$Cl$_2$·2H$_2$O system, the enthalpy and temperature sequences are at variance. The ΔH_L sequence is consistent with the steric order, whilst the temperature data suggest the importance of inductive factors. The $\Delta\nu_{C=O}$ sequence, *nmf* (16 cm^{-1}) <*aa* (21 cm^{-1})<*nma* (30 cm^{-1}) confirms the inductive order. Explanation of this apparent anomaly is difficult, owing largely to the lack of thermal data for the Ni(*nma*)$_2$Cl$_2$·2H$_2$O complex.

For the decomposition of the CuL$_2$Cl$_2$ complexes, lower T_e and T_{max} values were obtained for the complex with the more basic ligand, *aa*($\Delta\nu_{C=O}\approx 19$ cm^{-1}) compared with the *fa* complex ($\Delta\nu_{C=O}\sim$ 5 cm^{-1}). This is consistent with steric hindrance caused by the methyl-substituent in acetamide.

In the CoL$_2$Cl$_2$ system, only Co(*fa*)$_2$Cl$_2$ decomposed according to reactions Eqs. (1) and (2). However, Co(*fa*)$_2$Cl$_2$, Cu(*fa*)$_2$Cl$_2$, Cu(*aa*)$_2$Cl$_2$ and

$\mathrm{Ni}(aa)_2\mathrm{Cl}_2$ have similar structures. The T_e and T_max values for reaction Eq. (1) indicate the stability orders: (i) loss of *fa*, $\mathrm{Cu}(fa)_2\mathrm{Cl}_2 < \mathrm{Co}(fa)_2\mathrm{Cl}_2$; (ii) loss of *aa*, $\mathrm{Cu}(aa)_2\mathrm{Cl}_2 < \mathrm{Ni}(aa)_2\mathrm{Cl}_2$. A possible explanation for the low thermal stability of the copper(II) complexes is the very distorted octahedral structure.

4.1.2. Reactions of Set (2)

Thermal data for reaction 2b, Table 4, indicate the trends of $\mathrm{Ni}_3\mathrm{L}_2\mathrm{Cl}_6$: (i)$T_\mathrm{e}$ *pa<def<dmf<dma<nef*; (ii)T_max *pa<def<dma<dmf<nef*; (iii))ΔH_L *def≅pa≅ dma<nef<dmf*. Lower ΔH_L values for the complexes with *def*, *dma* or *pa*, compared to *nef* or *dmf*, are excellent evidence for the importance of steric hindrance caused by bulkier alkyl-substituent groups.

The ν_1 values (Table 2) suggest an interplay between steric and inductive factors. *pa* (7221 cm^{-1}) <*nef*(7232 cm^{-1})<*def*(7247 cm^{-1})< *dma*(7252 cm^{-1}) <*dmf* (7259 cm^{-1}). The sequence, *def<dma<dmf*, supports the steric order, while *nef<def*(<*dma*) can best be explained in terms of stronger inductive effects.

The T_e series, *pa<dmf<dma*, suggests the importance of inductive effects $\Delta\nu_{\mathrm{C=O}}$ data in Table 3 confirm this order: *pa* (9 cm^{-1})<*nef* (14 cm^{-1})<*dmf* (18 cm^{-1})≅ *dma* (19 cm^{-1})<*def* (29 cm^{-1}). The T_max series, *def<dma<dmf<nef*, is consistent with the importance of steric effects, while *pa<def* can best be justified in terms of stronger inductive effects. Results for the $\mathrm{Ni}_3\mathrm{L}_2\mathrm{Cl}_6$ system therefore suggest that the quantities ΔH_L, T_e and T_max indicate an interplay between the steric and the inductive factors.

T_e and T_max for reaction Eq. (3) and ΔH_L for reactions Eqs. (3) and (4), Table 4, indicate the orders of $\mathrm{NiL}_2\mathrm{Cl}_2$: (i)$T_\mathrm{e}$ and T_max *dmf<nef<pa<ba≅iba <fa*; (ii)ΔH_L *iba≅ba<pa*≅nef<*dmf<fa*. ΔH_L generally decreases with increase in size of the alkyl-substituent groups. Apart from the complex with *fa*, T_e and T_max generally increase with increase in basicity of the ligands. This is compatible with the inductive order produced by the $\Delta\nu_{\mathrm{C=O}}$ data: *pa* (8 cm^{-1})<*ba* (15 cm^{-1})<*iba* (18 cm^{-1}) ≅*nef* (20 cm^{-1})<*dmf* (23 cm^{-1}).

The $\mathrm{Ni}(dmf)_2\mathrm{Cl}_2$ and $\mathrm{Co}(dmf)_2\mathrm{Cl}_2$ complexes have different structures: octahedral and tetrahedral coordinations, respectively.

4.1.3. Reactions of Sets (3) and (4)

Within set (3), no reasonable solid-state stability comparison is feasible. $\mathrm{Co}(dma)_2\mathrm{Cl}_2$ showed a unique decomposition stoichiometry, while $\mathrm{Ni}_3(dmp)\mathrm{Cl}_6$ and $\mathrm{Co}_3(dma)\mathrm{Cl}_6$ contain different ligands and have octahedral and tetrahedral structures, respectively. Referring to set (4), $\mathrm{Co}(nma)_2\mathrm{Cl}_2$ and $\mathrm{Cu}(iba)_2\mathrm{Cl}_2$ exhibited octahedral structures, but with different amide ligands. $\mathrm{Co}(dmp)_2\mathrm{Cl}_2$ has a tetrahedral structure.

4.2. Comparison between the results of the present study and other related studies

House et al. [44] reported ΔH values for the CdCl_2-*picoline* system that were higher than those for the CdCl_2–*pyridine* system. The authors accounted for the higher values on the grounds that methylpyridine is more basic than pyridine. From studies of the NiCl_2–*imidazole* system, Losada et al. [53,54] reported that *N*-methylimidazole was held more strongly than imidazole and explained this in terms of the greater basicity of *N*-methylimidazole. In contrast, Farran et al. [5] reported a decrease in T_e values with increasing basicity of alkyl-substituted pyridine ligands in $\mathrm{PdL}_2\mathrm{Cl}_2$ complexes. The observed T_e order was explained [5] in terms of a *trans* influence of one ligand, which can cause the first ligand to be lost more easily. Results of the present study do not support the enhancement of thermal quantities with increasing basicity of the amides. Instead, steric factors appear to play a more important role in determining the magnitudes of ΔH_L, T_e and T_max. No simple relationship was found between ν_1 or $\Delta\nu_{\mathrm{C=O}}$ and the thermal quantities.

References

[1] P.A.B. Carstens, T.P. Knoetze, C.P.J. van Vuuren, Thermochim. Acta 128 (1988) 237.
[2] G. Siracusa, L. Abate, R. Maggiore, Thermochim. Acta 56 (1982) 333.
[3] G. Beech, J. Chem. Soc. A (1969) 1903.
[4] R.P. Bonomo, S. Gurrieri, S. Musumeci, E. Rizzarelli, G. Siracusa, Thermochim. Acta 9 (1974) 373.
[5] R. Farran, J.E. House, J. Inorg. Nucl. Chem. 34 (1972) 2219.
[6] A. Akhavein, J.E. House, J. Inorg. Nucl. Chem. 32 (1970) 1479.
[7] D.A. Thornton, P.F.M. Verhoeven, H.O. Desseyn, H. Hofmans, Thermochim. Acta 113 (1987) 161.

[8] H. Langfelderova, J. Thermal Anal. 12 (1977) 413.
[9] C. Van Dam, G. Hakvoort, J.C. Jansen, J. Reedijk, J. Inorg. Chem. 37 (1975) 713.
[10] S. Gurrieri, R. Maggiore, S. Musumeci, G. Siracusa, Thermochim. Acta 11 (1975) 73.
[11] S.H.J. De Beukeleer, H.O. Desseyn, S.P. Perlepes, J. Mullens, Thermochim. Acta 257 (1995) 149.
[12] J.R. Allan, A.D. Paton, K. Turvey, Thermochim. Acta 196 (1992) 391.
[13] J.R. Allan, B. McCloy, A.D. Paton, W.E. Smith, D.L. Gerrard, Thermochim. Acta 205 (1992) 127.
[14] M.E. Stone, B.E. Robertson, E. Stanley, J. Chem. Soc. A (1971) 3632.
[15] W.E. Bull, S.K. Madan, J.E. Willis, J. Inorg. Chem. 2 (1963) 303.
[16] M.E. Stone, K.E. Johnson, Can. J. Chem. 51 (1973) 1260.
[17] A.N. Nelwamondo, D.J. Eve, M.E. Brown, Thermochim. Acta, pp. 186 (this issue).
[18] E. Jona, V. Jesenak, T. Sramko, J. Gazo, J. Thermal Anal. 5 (1973) 57, 389.
[19] R.P. Bonomo, S. Gurrieri, S. Musumeci, E. Rizzarelli, G. Siracusa, Thermochim. Acta 10 (1974) 119.
[20] V.A. Logvinenko, O.V. Gegola, L.I. Myachina, J. Thermal Anal. 14 (1978) 265.
[21] J.R. Allan, D.H. Brown, R.H. Nuttal, D.W.A. Sharp, J. Inorg. Nucl. Chem. 27 (1965) 1529.
[22] R.S. Drago, D.W. Meek, M.D. Joesten, L. Laroche, Inorg. Chem. 2 (1963) 124.
[23] A.H. Gropp, H. Letaw, J. Chem. Phys. 21 (1953) 1621.
[24] M. Goldstein, W.D. Unsworth, Spectrochim. Acta 28A (1972) 1297.
[25] S. Mitra, G. De, N.R. Chaudhuri, Thermochim. Acta 66 (1983) 187.
[26] A.B.P. Lever, Inorganic Electronic Spectroscopy, Elsevier, London, 1968, Ch. 9.
[27] W.R. Hertler, E.L. Muetterties, Inorg. Chem. 5 (1966) 160.
[28] R.J.H. Clark, C.S. Williams, Inorg. Chem. 4 (1965) 350.
[29] R.H. Nuttal, Talanta 15 (1968) 157.
[30] D.M.L. Goodgame, M. Goodgame, M.J. Weeks, J. Chem. Soc. (1964) 5194.
[31] M. Goldstein, F.B. Taylor, W.D. Unsworth, J. Chem. Soc. Dalton (1972) 418.
[32] S.K. Madan, A.M. Donohue, J. Inorg. Nucl. Chem. 28 (1966) 1617.
[33] C.S. Kraihanzel, S.C. Grenda, Inorg. Chem. 4 (1965) 1037.
[34] R.J. Pace, J. Williams, R.L. Williams, J. Chem. Soc. (1961) 2196.
[35] S.C. Jain, R. Rivest, Can. J. Chem. 45 (1967) 139.
[36] M.A.J. Jungbauer, C. Curran, Nature 202 (1964) 290.
[37] M. Goldstein, W.D. Unsworth, Inorg. Chim. Acta 4 (1970) 432.
[38] I.A. Dorrity, K.G. Orrell, J. Inorg. Nucl. Chem. 36 (1974) 230.
[39] R.J.H. Clark, Spectrochim. Acta 21 (1965) 955.
[40] J.R. Allan, D.H. Brown, R.H. Nuttal, D.W.A. Sharp, J. Chem. Soc. A (1966) 1031.
[41] B.R. Carson, G. Kenessey, J.R. Allan, G. Liptay, J. Thermal Anal. 45 (1995) 369.
[42] J.R. Allan, B.R. Carson, D.L. Gerrard, S. Hoey, Thermochim. Acta 153 (1989) 173.
[43] J.R. Allan, D.H. Brown, R.H. Nuttal, D.W.A. Sharp, J. Inorg. Nucl. Chem. 27 (1965) 1865.
[44] J.E. House, A.L. Rohner, Thermochim. Acta 19 (1977) 119.
[45] J.R. Allan, G.M. Baillie, J. Thermal Anal. 14 (1978) 291.
[46] G. Beech, C.T. Mortimer, J. Chem. Soc. A (1967) 1111.
[47] G. Beech, C.T. Mortimer, E.G. Tyler, J. Chem. Soc. A (1967) 925.
[48] G. Liptay, G. Nagy, A. Borbely-Kuszmann, Thermochim. Acta 93 (1985) 97.
[49] G. Liptay, A. Borbely-Kuszmann, G. Nagy, J. Thermal Anal. 32 (1987) 91.
[50] G. Beech, C.T. Mortimer, E.G. Tyler, J. Chem. Soc. A (1969) 512.
[51] G. Beech, C.T. Mortimer, J. Chem. Soc. A (1967) 1115.
[52] A.B.P. Lever, J. Chem. Soc. (1963) 5042.
[53] M. Sachez, J. Losada, J. Thermal Anal. 28 (1983) 381.
[54] J. Losada, M. Sanchez, M. J Gonzalez, M. Moran, J. Inorg. Nucl. Chem. 43 (1981) 2269.